ISSN 1392–1320 MATERIALS SCIENCE (MEDŽIAGOTYRA). Vol. 27, No. 4. 2021

Thermal Performances and Fluidity of Biodegradable Poly(L-lactic acid) Filled with *N, N′*-Oxalyl Bis(piperonylic acid) Dihydrazide as a Nucleating Agent

Lisha ZHAO, Yanhua CAI *

Chongqing Key Laboratory of Environmental Materials & Remediation Technologies, Chongqing University of Arts and Sciences, Chongqing-402160, P.R. China

crossref http://dx.doi.org/10.5755/j02.ms.25139

Received 23 January 2020; accepted 22 February 2020

N, N′-oxalyl bis(piperonylic acid) dihydrazide (PAOD) was obtained through the amination of piperonylic acid chloride and its structure was characterized by Fourier transform infrared spectrometer and nuclear magnetic resonance. Melting blend technology was used to prepare the modified poly(L-lactic acid) (PLLA) containing the various loading PAOD as a new organic nucleating agent. The thermal performances including crystallization, melting behavior and thermal decomposition process, as well as the fluidity of PAOD-nucleated PLLA were investigated *via* a series of tests. The DSC results showed that, in comparison to DSC curve of the virgin PLLA, the DSC curves of all PLLA/PAOD appeared the sharp melt-crystallization peak, and a higher PAOD concentration caused the melt-crystallization to occur in the higher temperature region and reduced the negative effect of the high cooling rate on the melt-crystallization process. However, with increasing of PAOD concentration, the cold-crystallization enthalpy decreased from 24.4 J/g to 16.7 J/g. The melting peak after melt-crystallization depended on the heating rate and the PAOD concentration; and the double melting peaks appeared after isothermal crystallization in low temperature region was thought to be due to the melting-recrystallization. The addition of PAOD decreased the onset decomposition temperature of PLLA, but the onset decomposition temperature was determined by the PAOD concentration and the intermolecular interaction of PLLA and PAOD. Additionally, the PAOD could considerably improve the fluidity of PLLA.

Keywords: PLLA, nucleating agent, thermal performance, piperonylic acid.

1. INTRODUCTION

White pollution, originated from the waste plastics such as Polypropylene (PP), Polyvinyl chloride (PVC), Polystyrene (PS), etc., has led to more and more serious environmental pollution. Developing degradable bio-based polymer to replace the aforementioned non-degradable petroleum-based polymer is a good way of reducing the "white pollution". Poly(L-lactic acid) (PLLA), as a typical biodegradable polymer, has dominated both R&D and production comparing with other biodegradable polymers due to its biodegradability, compatibility, easy processibility, compostability, etc. These features promote PLLA to exhibit a promising application in drug release [1–3], 3D printing [4, 5], tissue engineering [6–8], etc. Especially the PLA is extensively used in packaging field [9, 10]. For instance, the solvent casting method was used to prepare the PLA biofilm containing the MgO nanoparticles. And these PLA/MgO films exhibited a larger tensile strength, and the better oxygen barrier and antibacterial efficacy comparing with the pristine PLA, indicating that the PLA/MgO film was an excellent food packaging material [11].

Unfortunately, PLLA suffers from an inhere defect of the slow crystallization rate [12, 13], leading to the long injection molding time, the poor heat resistance and low crystallinity, these performance deficiencies seriously restrict the large-scale usage of PLLA. Thus, overcoming this defect of the slow crystallization rate is very necessary to improve its performance and widen the usage of PLLA. And four typical methods were used to accelerate the crystallization of PLLA, they are increasing the amount of L-lactide isomers, adding nucleating agent or plasticizer, as well as playing with the molding conditions [14]. Compared to the three other methods, industrial production focus more on the adding nucleating agent in PLLA matrix, because a nucleating agent often possesses distinct advantages such as low dosage, easy operation, no overflow from matrix, low cost, etc. [15, 16]. A large number of compounds with different structures, like talc [17], calcium carbonate [18], zinc citrate [19], benzoylhydrazine derivatives [12, 20], amide derivatives [21, 22], etc., were employed to investigate their role in crystallization process of PLLA. Even so, it is still difficult to reveal the relationship between structure and nucleation effect for PLLA, whereas thoroughly revealing this relationship is very valuable to develop the efficient and commercial nucleating agents for PLLA. Under this circumstance, organic nucleating agents can exhibit a greater potential because of the molecular structure designability, better compatibility with PLLA and sufficient nucleation effect [23, 24]. Given that, in our previous works, we had designed and synthesized 1H-benzotriazole derivatives [25], isoniazid derivative [26] and hydrocinnamic acid derivatives [27] to serve as organic nucleating agents for PLLA, and these derivatives exhibited the excellent crystallization accelerating ability

* Corresponding author. Tel.: +86-23-61162815; fax: +86-23-61162725.
E-mail address: *caiyh651@aliyun.com* (Y.H Cai)

for PLLA. For example, 3 wt.% *N, N′*-bis(benzoyl) dodecanedihydrazide could cause the half-time of crystallization of PLLA to decrease to 22.9 s at 115 °C; and the nucleation mechanism was attributed to the chemical nucleation [28].

In the current work, we further designed and synthesized a new compound *N, N′*-oxalyl bis(piperonylic acid) dihydrazide (PAOD) to firstly evaluate its nucleation effect on PLLA in detailed, and the melting behavior, thermal decomposition behavior and fluidity of PAOD-nucleated PLLA were further investigated by differential scanning calorimeter (DSC), thermogravimetric analysis (TGA) and melt index instrument. This work may be helpful to enrich the category of PLLA's nucleating agent and realize the relationship of the nucleating agent and performance.

2. EXPERIMENTAL

2.1. Materials

PLLA (trade name: 4032D) used in this study was produced by Nature Works LLC of USA, and the commodity indicators were the D content of 1.20 % and the M_w of 1.70×10^5 g/mol. All chemical reagents, including oxalyl dihydrazide, piperonylic acid, triethylamine, sulfur oxychloride and *N, N*-dimethylformamide (DMF), were purchased from Chongqing Huanwei Chemical Company.

2.2. Synthesis of PAOD

The synthetize of PAOD was performed as shown in Fig. 1. First, the piperonylic acid chloride was prepared through acylation reaction of piperonylic acid and sulfur oxychloride in the presence of a few drops of DMF as catalyst. Then, the 0.01 mol oxalyl dihydrazide and 3 ml triethylamine were dissolved in 120 ml DMF with stirring, and then the 0.02 mol piperonylic acid chloride was slowly added into the aforementioned mixed solution to be further stirred at ice bath for 1 h. After that, the mixed solution was heated up to 60 °C, and held at 60 °C for 4 h with stirring. Finally, the reaction mixture was poured into 300 mL water, and the precipitate was filtrated, followed by washing using water for 3 times. The resulting product was dried in vacuum at 35 °C for 24 h. Fourier Transform Infrared Spectrometer (FT-IR) υ: 3416.6, 3009.0, 1698.2, 1651.6, 1607.7, 1504.7, 1490.2, 1445.1, 1382.7, 1360.6, 1289.7, 1263.2, 1156.7, 1113.7, 1086.3, 1037.9, 929.2, 877.4, 823.7, 744.4 cm^{-1}. ^1H Nuclear Magnetic Resonance (^1H NMR) δ: ppm; 10.78 (s, 1H, NH), 10.29 (s, 1H, NH), 7.00~7.55 (m, 3H, Ar).

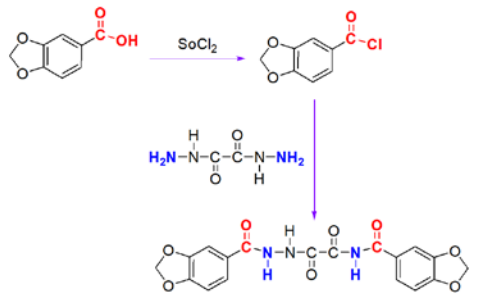

Fig. 1. Synthetic route of PAOD

2.3. Preparation of PLLA/PAOD sample

The modified PLLA containing the different PAOD concentration (0.5 wt.%, 1 wt.%, 2 wt.% and 3 wt.%) were prepared *via* the melt blending technology, and the relevant samples were marked as PLLA/0.5%PAOD, PLLA/1%PAOD, PLLA/2%PAOD and PLLA/3%PAOD, respectively. The detailed processing parameters were set as follow: the blending temperature was 190 °C, the blending time were 10 min at rotation speed of 32 rpm, and the mixture were further blended for 7 min at rotation speed of 64 rpm. After that, the mixture were hot pressed in a sheet with 0.4 mm thickness under 20 MPa for 7 min at 190 ºC, and further cool pressed under 20 MPa for 10 min at room temperature.

2.3. Characterization and testing

^1H NMR of the PAOD molecule was performed on a AVANCE 400 MHz nuclear magnetic resonance spectrometers, and the deuterium solvent was dimethyl sulphoxide during testing.

An IS50 spectrophoto meter was used to record the infrared spectra of PAOD molecule, and the testing wavenumber was from 4000 to 400 cm^{-1}. Additionally, the PAOD sample was mixed with KBr powders and pressed into a disk suitable for FT-IR measurement.

The melt-crystallization, cold-crystallization and melting process of the virgin PLLA and PAOD-nucleated PLLA were recorded by Q2000 DSC with 50 mL/min nitrogen. Before testing, the temperature and heat flow at different heating rate were calibrated using an indium standard.

Thermal decomposition behaviors of the virgin PLLA and PLLA/PAOD samples were investigate by Q500 TGA with 60 mL/min air. The testing temperature covered the range of 50 °C to 650 °C, and the heating rate was 5 ºC/min.

The fluidity of melting virgin PLLA and PLLA/PAOD samples were measured by the RTS0L400B melt index instrument (Beijing Guance Experimental Equipment Co., Ltd), and the measurement temperature was 180 °C, the load was 10 kg.

3. RESULTS AND DISCUSSION

3.1. Non-isothermal crystallization behavior

Usually, the non-isothermal crystallization behavior can directly estimate the crystallization accelerating effect of the nucleating agent for polymer. Fig. 2 showed the melt-crystallization DSC curves of the virgin PLLA and PLLA/PAOD samples from 190 ºC at a cooling rate of 1 ºC/min. It is clearly observed that the virgin PLLA can almost not form the non-isothermal crystallization peak in DSC curve, indicating that no crystals appear in cooling because of the poor crystallization ability of PLLA itself [29, 30]. In contrast with the virgin PLLA, all PLLA/PAOD samples have the significant and sharp non-isothermal crystallization peak, which illustrates that the introduction of PAOD accelerates the crystallization of PLLA in cooling, the primary reason is that the PAOD as a heterogeneous nucleating agent can supply enough

nucleation sites in PLLA matrix, which induces the occurrence of PLLA's crystallization in a high temperature range. Additionally, Fig. 2 also displays the influence of PAOD concentration on the melt-crystallization process of PLLA. With increasing of PAOD concentration from 0.5 wt.% to 3 wt.%, the melt-crystallization peak shifts toward the higher temperature, meaning that, as far as nucleation ability of PAOD in PLLA matrix, the 3 wt.% is still not the saturated concentration. However, it should be noted that the melt-crystallization peak only exhibits a very slight shift to the higher temperature, when the PAOD concentration is 2 wt.% ~ 3 wt.%. Overall, the addition of PAOD significantly promotes the crystallization of PLLA, and PLLA/3%PAOD sample has the highest onset crystallization temperature (T_{oc}) of 139.5 °C and melt-crystallization peak temperature (T_{mc}) of 135.9 °C, which are higher than these relevant values of other systems such as PLLA/DI [26], PLLA/CB [31] and PLLA/talc [32]. But the PLLA/2%PAOD sample exhibits the largest melt-crystallization enthalpy of 50.0 J/g (the crystallinity is 54.5 % according to the relevant equation [33, 34]).

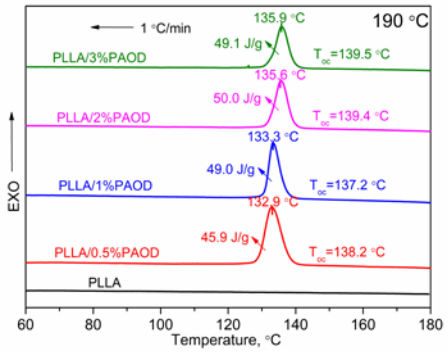

Fig. 2. Melt-crystallization DSC curves of the virgin PLLA and PLLA/PAOD samples at a cooling rate of 1 °C/min

Usually, the high temperature can arouse the molecular activity, and this high molecular activity may easily result in the intermolecular interaction. Fig. 3 displays the HOMO and LUMO of the PAOD and PLLA with 10 units obtained through the theoretical calculation of DMol3 (Task: Geometry Optimization, Quality: Medium, Use Symmetry), and the HOMO of PAOD and PLLA are –0.204 eV and –11.082 eV, the LUMO of PAOD and PLLA are –0.110 eV and 0.251 eV.

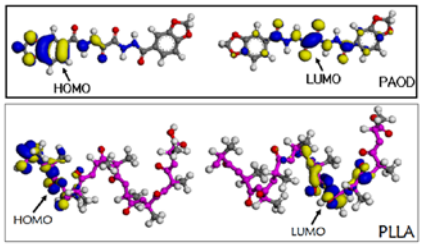

Fig. 3. HOMO and LUMO of PLLA and PAOD

According to the frontier molecular orbital theory, it is found that the LUMO-HOMO energy gap of 10.972 eV between PLLA and BADH is smaller than that of 11.333 eV of PLLA itself, meaning that the electron of PLLA easier flow to the LUMO of PAOD than the LUMO of PLLA during melt-blending process. Under this circumstance, the intermolecular interaction between PLLA and PAOD can be easily formed, and this interaction maybe used to explain the nucleation effect of PAOD for PLLA crystallization, that is, the nucleation mechanism maybe chemical nucleation.

As reported by other literature [35], the cooling rate plays an important role in melt-crystallization process of PLLA. Similarly, the influence of the cooling rate on the melt-crystallization behavior of PLLA was further investigated in this study. Fig. 4 is the melt-crystallization DSC curves of PLLA/PAOD sample at different cooling rates. It is clear that the melt-crystallization peak of any given sample shifts to the lower temperature with increasing of cooling rate, the reason is that a higher cooling rate causes the PLLA molecular segment to have no enough time to form the regular structure, as a result, the crystallization only occurs in a lower temperature region. In addition, an increase of cooling rate also makes the melt-crystallization peak become wider, in particular, the melt-crystallization peak of PLLA/0.5%PAOD sample only exhibits a shoulder peak, when the cooling rate is 10 ºC/min. However, the other PLLA/PAOD samples still possess the sharp melt-crystallization peak in the same circumstance. These results show that an increase of cooling rate must weaken the crystallization ability of PLLA/PAOD system, especially the effect of a higher cooling rate on the melt-crystallization of PLLA containing a small amount of PAOD (such as 0.5 wt.%) is very negative.

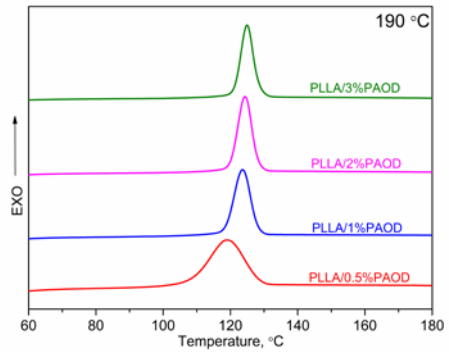

a

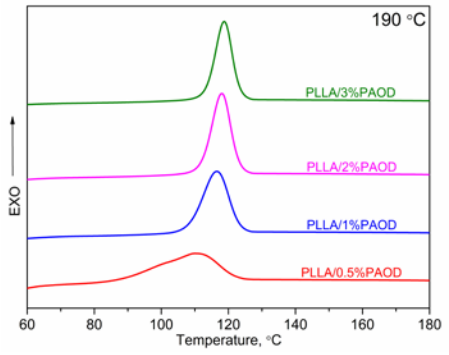

b

Fig. 4. Melt-crystallization behavior of PLLA/PAOD sample from 190 ºC at different cooling rates: a – 5 °C/min; b – 10 ºC/min)

As shown in Fig. 4, it is a fact that, when a cooling rate is determined, the melt-crystallization peak shifts

toward the higher temperature with increasing of PAOD concentration, that is, the influence trend of PAOD concentration on the crystallization process of PLLA does not depend on the cooling rate. Apart from the melt-crystallization, non-isothermal crystallization also includes the cold-crystallization process. Thus, the cold-crystallization behavior of PLLA/PAOD sample was also studied. Fig. 5 is the cold-crystallization DSC curves of PLLA/PAOD sample at a heating rate of 1 °C/min. In contrast with the melt-crystallization process, the cold-crystallization peak moves toward the lower temperature with increasing of PAOD concentration, and the cold-crystallization enthalpy decreases from 24.4 J/g to 16.7 J/g.

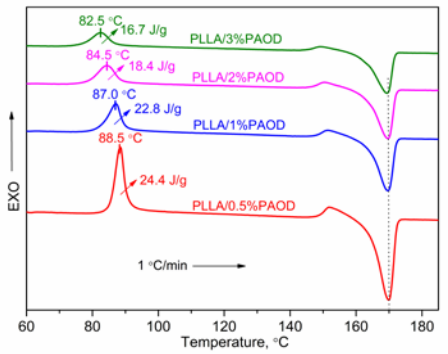

Fig. 5. Cold-crystallization DSC curves of PLLA/PAOD samples at a heating rate of 1 °C/min

Moreover, the cold-crystallization peak gradually become wider. The probable reason is that a larger amount of PAOD and PLLA itself can provide more nucleation sites, resulting in very fast nuclear rate, and the crystallization is induced to occur at a lower temperature. However, on the other hand, a larger amount of PAOD have the more serious inhibition for the mobility of PLLA molecular chain, which leads to appearance of the wider peak. In a word, the addition of PAOD exhibits the greater hindrance effect for PLLA's cold-crystallization.

3.2. Melting behavior

Fig. 6 is the melting behaviors of PLLA/PAOD system at different heating rates after melt-crystallization at a cooling rate of 1 °C/min. With increasing of the heating rate, the melting range of a given PLLA/PAOD sample becomes wider due to the thermal inertia. However, as seen in Fig. 6, at any given heating rate, the melting peak of PLLA containing a lower loading of PAOD appears at a higher temperature region, meaning that PLLA with a small amount of PAOD possesses the more perfect crystals in cooling, the reason is that the existence of a larger amount of PAOD in PLLA matrix must lead to the higher nucleation density, under this circumstance, more small crystal based on these nucleation sites can be formed and get growth. Inevitably, these crystals impinge on their neighbors during growth, finally resulting in the appearance of more imperfect crystals. In addition, it is possible to occur the recrystallization at a low heating rate in heating, because only about 54 % crystallization was completed in cooling as mentioned in non-isothermal crystallization section. As a result, when the heating rate is 1 °C/min, both PLLA/2%PAOD and PLLA/3%PAOD exhibit the double-melting peaks, but the high-temperature melting peaks are very weak, indicating that only tiny amount of crystals are formed in the second heating, which further confirms the powerful nucleation ability of PAOD for PLLA.

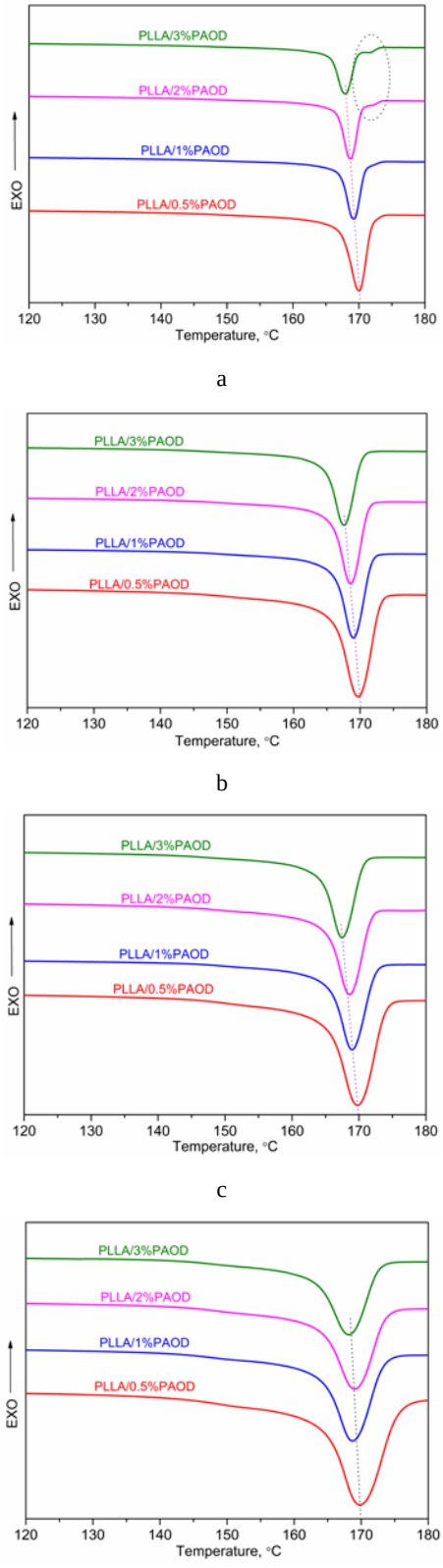

Fig. 6. Melting behavior of PLLA/PAOD samples at different heating rates after cooling of 1 °C/min: a – 1 °C/min; b – 3 °C/min; c – 5 °C/min; d – 10 °C/min

A comparative study on melting behavior of PLLA/PAOD samples at a heating rate of 10 °C/min after isothermal crystallization at 105 °C and 135 °C for different time was further performed using DSC (See Fig. 7). It is clear that Fig. 7 exhibits the different melting DSC curves because of the different crystallization temperatures, showing that the isothermal crystallization temperature significantly affects the following melting behavior.

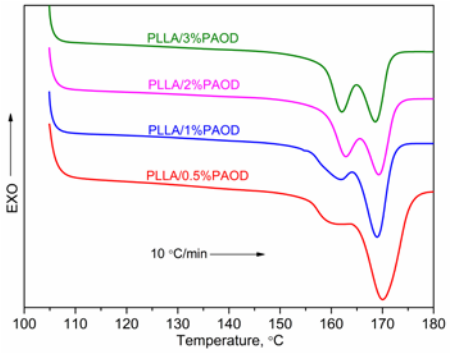

a

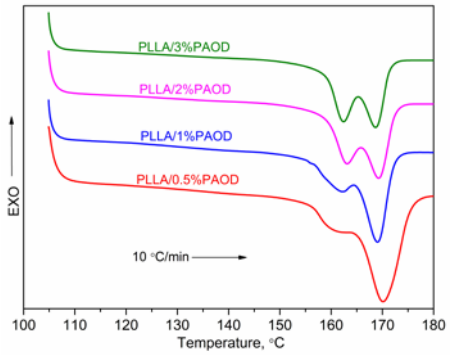

b

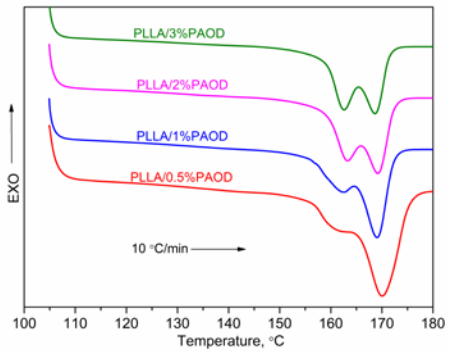

c

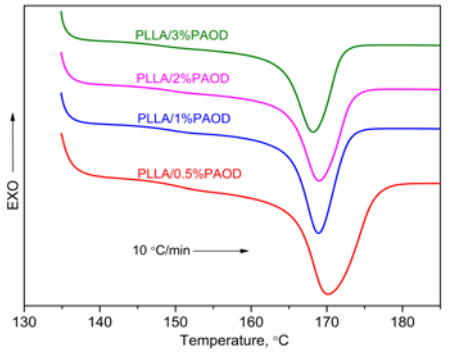

d

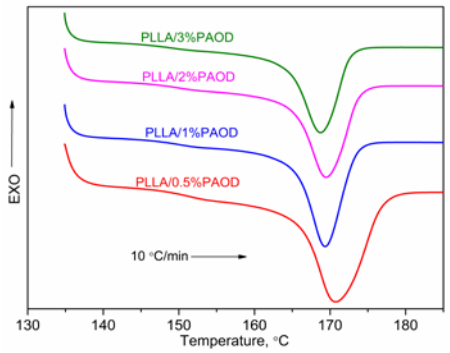

e

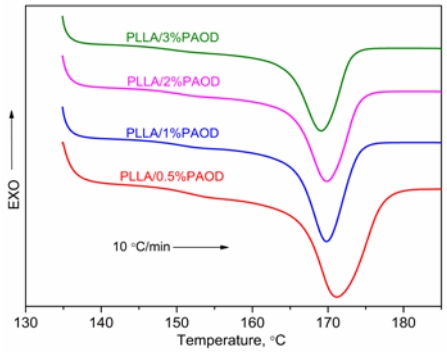

f

Fig. 7. Melting behavior of PLLA/PAOD samples at a heating rate of 10 °C/min after isothermal crystallization: a – 105 °C for 60 min; b – 105 °C for 120 min; c – 105 °C for 180 min; d – 135 °C for 60 min; e – 135 °C for 120 min; f – 135 °C for 180 min

When the crystallization temperature is 105 °C, all PLLA/PAOD samples exhibit the double-melting peaks; What is more, it is found that the low-temperature melting peak and high-temperature melting peak of a given PLLA/PAOD sample are located in the same temperature region in DSC curve, as well as the melting curve profile is also very similar, meaning that the effect of crystallization time on the melting behavior of a given PLLA/PAOD sample after isothermal crystallization is neglectable. That is to say, PLLA/PAOD systems has obtained the corresponding maximum crystallinity after isothermal crystallization at 105 °C for 60 min, resulting in that the low-temperature melting peak appears in the same temperature region; whereas a same heating rate in heating causes the high-temperature to locate the same position. This result effectively evidences that the double-melting peaks behavior of PLLA/PAOD samples is assigned to melting-recrystallization [36]. However, for the melting process of PLLA/PAOD samples after isothermal crystallization at 135 °C, all PLLA/PAOD samples exhibit only the single melting peak, and the melting curves do still not depend on the crystallization time.

3.3. Thermal stability and fluidity

Thermal decomposition temperature as an ultimate-usage temperature index characterized the thermal stability of plastic products, especially investigating on the thermal stability under air is very necessary to practical application. Fig. 8 is the TGA curves of the virgin PLLA and PLLA/PAOD samples at a heating rate of 5 °C/min under

air. Evidently all PLLA/PAOD samples as the virgin PLLA only exhibit one thermal decomposition stage, indicating that the thermal decomposition profile of PLLA does not depend on the PAOD, possibly resulting from the limited dosage of PAOD in PLLA matrix. And it is found from Fig. 8 that the weightlessness is situated in the range of 300 ~ 370 °C, stemming from the chain scissions and loss of ester groups [16, 37]. Although the addition of PAOD cannot change the decomposition profile of PLLA, the effect of PAOD and its concentration on the onset thermal decomposition temperature (T_{od}) is neglectable. And the T_{od} of the virgin PLLA, PLLA/0.5%PAOD, PLLA/1%PAOD, PLLA/2%PAOD and PLLA/3%PAOD are 341.3 °C, 331.2 °C, 326.9 °C, 336.4 °C and 328.1 °C, respectively. Through T_{od} data analysis, the T_{od} of all PLLA/PAOD samples are lower than that of the virgin PLLA, meaning that the addition of PAOD reduces the thermal stability of PLLA. However, it is also found that the T_{od} does not exhibit a linear decrease with increasing of PAOD concentration, and PLLA/2%PAOD has the largest T_{od} value of 336.4 °C comparing with other PLLA/PAOD samples, resulting from the competitive relationship between intermolecular interaction and low melting temperature of PAOD. That is, a larger amount of PAOD must lead to a lower decomposition temperature because of the low decomposition temperature of PAOD itself; but a larger amount of PAOD in PLLA matrix may also form the stronger interaction from C=O of PLLA and N–H of PAOD. If the interaction was predominant over the low melting temperature of PAOD, the PLLA/PAOD system can exhibit a high T_{od}; on the contrary, there exists a low T_{od}.

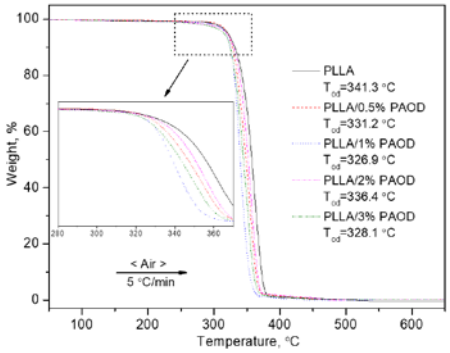

Fig. 8. TGA curves of the virgin PLLA and PLLA/PAOD

For practical manufacturing, the fluidity is often used to estimate the processing difficulty of polymer modified using various additives. Further for fluidity, the measurement of the melt flow rate (MFR) can directly characterizes the fluidity of polymers or the modified polymers. Usually, the larger the MFR value is, the better the fluidity is. Fig. 9 is the MFR of the virgin PLLA and PLLA/PAOD samples. As shown in Fig. 9, the addition of PAOD considerably improves the fluidity of PLLA, because all PLLA/PAOD samples have the larger MFR than the virgin PLLA. Furthermore, the MFR value continuous increases with increasing of PAOD concentration. Even the MFR of PLLA/3%PAOD is up to 12.9 g/10 min, which is about 7.7 times with respect to virgin PLLA.

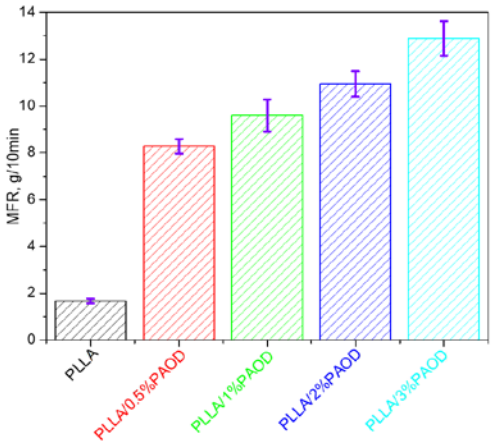

Fig. 9. MFR of the virgin PLLA and PLLA/PAOD samples

4. CONCLUSIONS

In this work, PAOD as a new nucleating agent was used to accelerate the crystallization of PLLA, and the other effects including melting behavior, thermal stability and fluidity were further investigated. The melt-crystallization process indicated that the PAOD could significantly accelerate the crystallization of PLLA in cooling, and increasing the PAOD concentration could make the melt-crystallization peak shift toward the higher temperature, and the PLLA/3%PAOD had the highest T_{oc} and T_{mc}, but the PLLA/2%PAOD possessed the largest melt-crystallization enthalpy. An increase of the cooling rate promoted the melt-crystallization peak to move toward the lower temperature and become wider, meaning that a higher cooling rate had a larger negative effect on the crystallization ability of PLLA/PAOD samples. In contrast with the melt-crystallization, the cold-crystallization peak shifted toward the lower temperature with increasing of PAOD concentration. For the melting process after melt-crystallization at cooling of 1 °C/min, the PAOD concentration and heating rate were two important factors; and an increase of heating rate could lead to the wider melting peak, as well as the melting peak of PLLA containing a larger amount of PAOD appeared at the lower temperature. The effect of the crystallization temperature on the melting peak was significant, and the double melting peaks appeared after isothermal crystallization in low temperature region resulted from the melting-recrystallization. Although the PAOD could not almost change the thermal decomposition profile of PLLA, overall, the addition of PAOD decreased the thermal stability of PLLA, whereas the drop in T_{od} depended on the PAOD concentration and the interaction between PLLA and PAOD. Finally, the influence of PAOD on the MFR was positive, showing the better fluidity.

Acknowledgments

This work was supported by National Natural Science Foundation of China (project number 51403027), Natural Science Foundation of Chongqing Municipal Science and Technology Commission (project number cstc2015jcyjBX0123 and cstc2019jcyj-msxmX0876), Scientific and Technological Research Program of Chongqing Municipal Education Commission

(KJQN201801319), and Foundation of Yongchuan District (project number Ycstc, 2018cc0801).

REFERENCES

1. **Yang, F.H., Niu, X.F., Gu, X.N., Xu, C.P., Wang, W., Fan, Y.B.** Biodegradable Magnesium-incorporated Poly(L-lactic acid) Microspheres for Manipulation of Drug Release and Alleviation of Inflammatory Response *ACS Applied Materials & Interfaces* 11 (26) 2019: pp. 23546 – 23557. https://doi.org/10.1021/acsami.9b03766
2. **Varga, N., Turcsanyi, A., Hornok, V., Csape, E.** Vitamin E-loaded PLA- and PLGA-based Core-shell Nanoparticles: Synthesis, Structure Optimization and Controlled Drug Release *Pharmaceutics* 11 (7) 2019: pp. 0357.1 – 0357.14. https://doi.org/10.3390/pharmaceutics11070357
3. **Takasaki, M., Nakashima, K., Tsuruda, R., Tokuda, T., Tanaka, K., Kobayashi, H.** Drug Release Behavior of a Drug-loaded Polylactide Nanofiber Web Prepared via Laser-electrospinning *Journal of Macromolecular Science Part B-Physics* 58 (6) 2019: pp. 592 – 602. https://doi.org/10.1080/00222348.2019.1615193
4. **Ecker, J.V., Haider, A., Burzic, I., Huber, A, Eder, G., Hild, S.** Mechanical Properties and Water Absorption Behavior of PLA and PLA/Wood Composites Prepared by 3D Printing and Injection Moulding *Rapid Prototyping Journal* 25 (4) 2019: pp. 672 – 678. https://doi.org/10.1108/RPJ-06-2018-0149
5. **Sang, L., Han, S.F., Li, Z.P., Yang, X.L., Hou, W.B.** Development of Short Basalt Fiber Reinforced Polylactide Composites and Their Feasible Evaluation for 3D Printing Applications *Composites Part B-Engineering* 164 2019: pp. 629 – 639. https://doi.org/10.1016/j.compositesb.2019.01.085
6. **Luo, W.H., Cheng, L.H., Yuan, C.X., Wu, Z.P., Yuan, G.M., Hou, M.X., Chen, J.Y., Luo, C.Y., Li, W.** Preparation, Characterization and Evaluation of Cellulose Nanocrystal/Poly(lactic acid) in situ Nanocomposite Scaffolds for Tissue Engineering *International Journal of Biological Macromolecules* 134 2019: pp. 469 – 479. https://doi.org/10.1016/j.ijbiomac.2019.05.052
7. **Mao, D.Y., Li, Q., Li, D.K., Chen, Y.S., Chen, X.H., Xu, X.** Fabrication of 3D Porous Poly(lactic acid)-based Composite Scaffolds with Tunable Biodegradation for Bone Tissue Engineering *Materials & Design* 142 2018: pp. 1 – 10. https://doi.org/10.1016/j.matdes.2018.01.016
8. **Abu Ghalia, M., Dahman, Y.** Fabrication and Enhanced Mechanical Properties of Porous PLA/PEG Copolymer Reinforced with Bacterial Cellulose Nanofibers for Soft Tissue Engineering Applications *Polymer Testing* 61 2017: pp. 114 – 131. https://doi.org/10.1016/j.polymertesting.2017.05.016
9. **Wang, H.L., Liu, H., Chu, C.J., She, Y., Jiang, S.W., Zhai, L.F., Jiang, S.T., Li, X.J.** Diffusion and Antibacterial Properties of Nisin-loaded Chitosan/poly(L-lactic acid) Towards Development of Active Food Pacjaging Film *Food and Bioprocess Technology* 8 (8) 2015: pp. 1657 – 1667. https://doi.org/10.1007/s11947-015-1522-z
10. **Swaroop, C., Shukla, M.** Development of Blown Polylactic acid-MgO Nanocomposite Films for Food Packaging *Composites Part A-Applied Science and Manufacturing* 124 2019: pp. 105482.1-105482.9. https://doi.org/10.1016/j.compositesa.2019.105482
11. **Swaroop, C., Shukla, M.** Nano-magnesium Oxide Reinforced Polylactic Acid Biofilms for Food Packaging Applications *International Journal of Biological Macromolecules* 113 2018: pp. 729 – 736. https://doi.org/10.1016/j.ijbiomac.2018.02.156
12. **Fan, Y.Q., Yan, S.F., Yin, J.B.** The Relationship Between Solubility and Nucleating Effect of Organic Nucleating Agent in Poly(L-lactic acid) *Journal of Applied Polymer Science* 136 2019: pp. 46851.1 – 46851.11. https://doi.org/10.1002/app.46851
13. **Tan, H., Wang, H.Q., Tang, Y., Zhang, S.Y., Yang, W., Liu, Z.Y., Yang, M.B.** Preparation of Functionalized Cellulose Nanoparticles and Their Effect on the Crystallization Behaviors of Poly(L-lactide) Based Nanocomposites *Polymer Interantional* 67 (11) 2018: pp. 1535 – 1544. https://doi.org/10.1002/pi.5675
14. **Cai, Y.H., Yan, S.F., Fan, Y.Q., Yu, Z.Y., Chen, X.S., Yin, J.B.** The Nucleation Effect of *N, N′*-Bis(benzoyl) Alkyl Diacid Dihydrazide on Crystallization of Biodegradable Poly(L-lactic acid) *Iranian Polymer Journal* 21 (7) 2012: pp. 435 – 444. https://doi.org/10.1007/s13726-012-0046-x
15. **Xu, X.K., Zhen, W.J., Bian, S.Z.** Structure, Performance and Crystallization Behavior of Poly(lactic acid)/Humic Acid Amide Composites *Polymer-Plastics Technology and Engineering* 57 (18) 2018: pp. 1858 – 1872. https://doi.org/10.1080/03602559.2018.1434670
16. **Zhao, L.S., Cai, Y.H.** Investigating the Physical Properties of Poly(L-lactic acid) Modified Using a Aromatics Succinic Dihydrazide Derivative *Polymer Science, Series A* 60 (6) 2018: pp. 777 – 787. https://doi.org/10.1134/S0965545X18070088
17. **Li, Y., Han, C.Y., Yu, Y.C., Xiao, L.G., Shao, Y.** Effect of Content and Particle Size of Talc on Nonisothermal Melt Crystallization Behavior of Poly(L-lactide) *Journal of Thermal Analysis and Calorimetry* 135 (4) 2019: pp. 2049 – 2058. https://doi.org/10.1007/s10973-018-7365-x
18. **Liang, J.Z., Zhou, L., Tang, C.Y., Tsui, C.P.** Crystalline Properties of Poly(L-lactic acid) Composites Filled with Nanometer Calcium Carbonate *Composites Part B-Engineering* 45 (1) 2013: pp. 1646 – 1650. https://doi.org/10.1016/j.compositesb.2012.09.086
19. **Teranishi, S., Kusumi, R., Kimura, F., Kimura, T., Aburaya, K., Maeyama, M.** Biaxial Magnetic Orientation of Zinc Citrate as Nucleating Agent of Poly(L-lactic acid) *Chemistry Letters* 46 (6) 2017: pp. 830 – 832. https://doi.org/10.1246/cl.170092
20. **Bai, H.W., Huang, C.M., Xiu, H., Zhang, Q., Fu, Q.** Enhancing Mechanical Performance of Polylactide by Tailoring Crystal Morphology and Lamellae Orientation with the Aid of Nucleating Agent *Polymer* 55 2014: pp. 6924 – 6934. https://doi.org/10.1016/j.polymer.2014.10.059
21. **Leone, N., Roy, M., Saidi, S., de Kort, G., Hermida-Merino, D., Wilsens, C.H.R.M.** Improving Processing, Crystallization, and Performance of Poly-L-lactide with an Amide-based Organic Compound as Both Plasticizer and Nucleating Agent *ACS Omega* 4 (6) 2019: pp. 10376 – 10387. https://doi.org/10.1021/acsomega.9b00848
22. **Shen, T.F., Xu, Y.S., Cai, X.X., Ma, P.M., Dong, W.F., Chen, M.Q.** Enhanced Crystallization Kinetics of Poly(lactide) with Oxalamide Compounds as Nucleators:

Effect of Space Length Between the Oxalamide Moieties *RSC Advances* 6 (54) 2016: pp. 48365 – 48374. https://doi.org/10.1039/c6ra04050k

23. **Zheng, L., Zhen, W.J.** Preparation and Characterization of Amidated Graphene Oxide and its Effect on the Performance of Poly(lactic acid) *Iranian Polymer Journal* 27 2018: pp. 239 – 252. https://doi.org/10.1007/s13726-018-0604-y
24. **Geng, Z.X., Zhen, W.J., Song, Z.B., Wang, X.F.** Structure and Performance of Poly(lactic acid)/Amide Ethylenediamine Tetraacetic Acid Disodium Salt Intercalation Layered Double Hydroxides Nanocomposites *Journal of Polymer Research* 25 2018: pp. 115.1 – 115.16. https://doi.org/10.1007/s10965-018-1482-x
25. **Cai, Y.H., Tang, Y., Zhao, L.S.** Poly(L-lactic acid) with Organic Nucleating Agent *N, N, N′*-Tris(1H-benzotriazole) Trimesinic Acid Acethydrazide: Crystallization and Melting Behavior *Journal of Applied Polymer Science* 132 (32) 2015: pp. 42402.1 – 42402.7. https://doi.org/10.1002/app.42402
26. **Cai, Y.H., Zhao, L.S., Tian, L.L.** Investigating the Crystallization, Melting Behavior, and Thermal Stability of Poly(L-lactic acid) Using Aromatic Isoniazid Derivative as Nucleating Agent *Polymer Bulletin* 74 (9) 2017: pp. 3751 – 3764. https://doi.org/10.1007/s00289-017-1923-4
27. **Zhao, L.S., Cai, Y.H., Liu, H.L.** *N, N′*-sebacic Bis(hydrocinnamic acid) Dihydrazide: A Crystallization Accelerator for Poly(L-lactic acid) *E-Polymers* 19 2019: pp. 141 – 153. https://doi.org/10.1515/epoly-2019-0016
28. **Cai, Y.H., Zhao, L.S.** The Effect of *N, N′*-bis(benzoyl) Dodecanedihydrazide on Enhancing the Crystallization Rate of Poly(L-lactic acid) *Polimery* 63 (11 – 12) 2018: pp. 815 – 820. https://doi.org/10.14314/polimery.2018.11.10
29. **Feng, Y.Q., Ma, P.M., Xu, P.W., Wang, R.Y., Dong, W.F., Chen, M.Q., Joziasse, C.** The Crystallization Behavior of Poly(lactic acid) with Different Types of Nucleating Agents *International Journal of Biological Macromolecules* 106 2018: pp. 955 – 962. https://doi.org/10.1016/j.ijbiomac.2017.08.095
30. **Zhang, J.F., Sun, X.Z.** Mechanical Properties and Crystallization Behavior of Poly(lactic acid) Blended with Dendritic Hyperbranched Polymer *Polymer International* 53 2004: pp. 716 – 722. https://doi.org/10.1002/pi.1457
31. **Su, Z.Z., Li, Q.Y., Liu, Y.J., Guo, W.H., Wu, C.F.** The Nucleation Effect of Modified Carbon Black on Crystallization of Poly(lactic acid) *Polymer Engineering and Science* 50 2010: pp. 1658 – 1666. https://doi.org/10.1002/pen.21621
32. **Cai, Y.H.** Crystallization and Melting Behavior of Biodegradable Poly((L-lactic acid)/Talc Composites *E-Journal of Chemistry* 9 (3) 2012: pp. 1569 – 1574. https://doi.org/10.1155/2012/570752
33. **Li, X.X., Yin, J.B., Yu, Z.Y., Yan, S.F., Lu, X.C., Wang, Y.J., Cao, B., Chen, X.S.** Isothermal Crystallization Behavior of Poly(L-lactic acid)/Organo-montmorillonite Nanocomposites *Polymer Composites* 30 2009: pp. 1338 – 1344. https://doi.org/10.1002/pc.20721
34. **Hong, Z.K., Zhang, P.B., He, C.L., Qiu, X.Y., Liu, A., Chen, L., Chen, X.S., Jing, X.B.** Nano-composite of Poly(L-lactide) and Surface Grafted Hydroxyapatite: Mechanical Properties and Biocompatibility *Biomaterials* 26 (32) 2005: pp. 6296 – 6304. https://doi.org/10.1016/j.biomaterials.2005.04.018
35. **Su, Z.Z., Guo, W.H., Liu, Y.J., Li, Q.Y., Wu, C.F.** Non-isothermal Crystallization Kinetics of Poly(lactic acid)/Modified Carbon Black Composite *Polymer Bulletin* 62 2009: pp. 629 – 642. https://doi.org/10.1007/s00289-009-0047-x
36. **Yasuniwa, M., Tsubakihara, S., Sugimoto, Y., Nakafuku, C.** Thermal Analysis of the Double-melting Behavior of Poly(L-lactic acid) *Journal of Polymer Science: Part B: Polymer Physics* 42 (1) 2004: pp. 25 – 32. https://doi.org/10.1002/polb.10674
37. **Elsawy, M.A., Saad, G.R., Sayed, A.M.** Mechanical, Thermal, and Dielectric Properties of Poly(lactic acid)/Chitosan Nanocomposites *Polymer Engineering and Science* 56 (9) 2016: pp. 987 – 994. https://doi.org/10.1002/pen.24328